

The detection of Broad Iron K and L line emission in the Narrow-Line Seyfert 1 Galaxy 1H 0707-495 using XMM-Newton

A.C. Fabian¹, A. Zoghbi¹, R.R. Ross², P. Uttley³, L.C. Gallo⁴, W.N. Brandt⁵, A. Blustin¹, T. Boller⁶, M.D. Caballero-Garcia¹, J. Larsson¹, J.M. Miller⁷, G. Miniutti⁸, G. Ponti⁹, R.C. Reis¹, C.S. Reynolds¹⁰, Y. Tanaka⁶ & A.J. Young¹¹

1. Institute of Astronomy, Madingley Road, Cambridge CB3 0HA, UK
2. Physics Department, College of the Holy Cross, Worcester, MA 01610, USA
3. School of Physics and Astronomy, University of Southampton, Highfield, Southampton SO17 1BJ, UK
4. Department of Astronomy and Physics, Saint Mary's University, Halifax, Nova Scotia, Canada
5. Department of Astronomy and Astrophysics, The Pennsylvania State University, 525 Davey Lab, University Park, PA 16802 USA
6. Max-Planck-Institut für Extraterrestrische Physik, Giessenbachstrae, Postfach 1312, 85741 Garching, Germany
7. Department of Astronomy, University of Michigan, Ann Arbor MI 48109, USA
8. Laboratorio de Astrofísica Espacial y Física Fundamental (CSIC-INTA), P.O. Box 78, E-28691, Villanueva de la Cañada, Madrid, Spain
9. Laboratoire APC, UMR 7164, 10 rue A. Domon et L. Duquet, 75205 Paris, France
10. Department of Astronomy and the Center for Theory and Computation, University of Maryland, College park, MD20742, USA
11. H. H. Wills Physics Laboratory, University of Bristol, Tyndall Avenue, Bristol BS8 1TL

Since the discovery of the first broad iron-K line in 1995 from the Seyfert Galaxy MCG-6-30-15¹, broad iron-K lines have been found in several other Seyfert galaxies², from accreting stellar mass black holes³ and even from accreting neutron stars⁴. The iron-K line is prominent in the reflection spectrum^{5,6} created by the hard X-ray continuum irradiating dense accreting matter. Relativistic distortion⁷ of the line makes it sensitive to the strong gravity and spin of the black hole⁸. The accompanying iron-L line emission should be detectable when the iron abundance is high. Here we report the first discovery of both iron-K and L emission, using XMM-Newton observations of the Narrow-

Line Seyfert 1 Galaxy⁹ 1H 0707-495. The bright Fe-L emission has enabled us, for the first time, to detect a reverberation lag of 30 s between the direct X-ray continuum and its reflection from matter falling into the hole. The observed reverberation timescale is comparable to the light-crossing time of the innermost radii around a supermassive black hole. The combination of spectral and timing data on 1H 0707-495 provides strong evidence that we are witnessing emission from matter within a gravitational radius, or a fraction of a light-minute, from the event horizon of a rapidly-spinning, massive black hole.

The galaxy 1H0707-495 has been observed several times by XMM-Newton^{10–12}. The first observation revealed a sharp and deep spectral drop at 7 keV in the rest frame (the source redshift is 0.041) but no narrow emission features. This led to two main interpretations¹⁰: either the source is partially obscured by a large column of iron-rich material or it has very strong X-ray reflection¹¹ in its innermost regions where relativistic effects modify the observed spectrum. In other words the sharp drop is either due to a photoelectric absorption edge, or the blue wing of a line partially shaped by relativistic Doppler shifts. The absorption origin requires that the iron abundance is about 30 times the Solar value (unless the spectrum is e-folding below 10 keV¹³, when the value is reduced), whereas reflection requires that this factor is between 5 and 10. The extreme variability of the source moreover appears to be due to changes mostly in the intensity of the powerlaw continuum, above 1 keV, which does not make sense in a partial covering model.

We have analysed the spectral variability of new observations of the source taken with XMM-Newton in January 2008. Variations from 1 to 12 ct s⁻¹ are seen over 4 XMM orbits. The difference spectrum between low and high flux states is well fitted by a powerlaw continuum with photon index $\Gamma = 3$, with an excess at lower (below 1.1 keV) energies. Strong skewed and broad residuals are seen above such a powerlaw fitted to the full source spectrum, peaking around 0.9 and 6.7 keV. The data are well described by a simple phenomenological model composed of a powerlaw continuum, a soft blackbody, two relativistically-broad (Laor¹⁴) lines and Galactic absorption (corresponding to $N_{\text{H}} = 5 \times 10^{20} \text{ cm}^{-2}$). We show the ratio of the

spectrum to the continuum in that model in Fig. 1. This ratio spectrum is clearly dominated by two strong broad emission lines. They are characterised by energies of 0.89 and 6.41 keV (in our frame), innermost radius of $1.3r_g$ ($1r_g = GM/c^2$), outermost radius of $400r_g$, an emissivity index of 4 and an inclination of 55.7 deg. The normalizations of the lines (in photon spectra) are in the ratio of 20:1 and their rest energies correspond well to ionized iron-L and K, respectively. We have tried a variety of continuum models and always obtain similar results. The data have also been fitted with a self-consistent model reflection spectrum¹⁵ (Fig. 2; see Supplementary Information for more details) which reproduces the correct relative fluxes for the lines. Iron is almost 9 times the Solar abundance value with the other elements at the Solar values. Perhaps a dense nuclear star cluster has led to the formation of massive white dwarf binaries which have enriched the nucleus with SN Ia ejecta rich in iron (such a scenario has been invoked in globular star clusters¹⁶).

The presence of broadened and skewed lines other than iron-K is an important prediction of the disk reflection model that we have now confirmed. Furthermore, we have shown that the relative strengths of the observed iron-L and iron-K lines agree well with predictions based on atomic physics. While it is possible to construct a partial-covering, absorption-dominated, model^{10,12} for the prominent K-shell iron feature, the L-shell absorption edge of ionized iron required around 1 keV is accompanied by an unacceptably strong absorption feature around 0.75 keV from an unresolved transition array of Fe IX-XI. Previous work^{10,12} on absorption models for 1H 0707-495 have been unable to account for the spectral structure around 1 keV without invoking emission. The strong variability, and shape, of this emission component points to the inner regions of the flow and thus to a reflection solution.

The source fractional rms variability is roughly constant below 1 keV, increases abruptly at 1 keV and then drops back to the soft level above 4 keV, in agreement with the expectation of the two-component model (reflection plus powerlaw) used to fit the data. Both components vary in amplitude but the powerlaw nearly twice as much. The non-linear behaviour of the variability in accreting black holes¹⁷ is considered

to be due to the cumulative random effects of the orbital variations from many radii effectively multiplied together. On the shortest time-scales light-crossing effects will become important, since the light path for the direct primary radiation is shorter than that for the reflected radiation. This effect is seen for the first time in the frequency-dependent lags, Fig. 3. The large positive lag for variations slower than 0.6 mHz (time-scales greater than 30 min) is probably due to the inward drift of accretion fluctuations through the emitting region¹⁸, causing the density and thus ionization state of the irradiated disc to respond first. Variations faster than 0.6mHz show a negative lag in the sense that the soft reflection dominated band follows the hard powerlaw dominated one by about 30 s. This is in the opposite sense to a Comptonization lag produced by upscattering of photons (or to any model where the spectral drop at 1 keV is instead produced by absorption which is responding to the changing continuum) and is explained by reverberation. If the lag time corresponds to the natural length of about hr_g , we expect h to be 2–5, then we deduce a mass for the black hole of about $7 \times 10^6 h^{-1} M_\odot$, which is reasonable for this source (no definitive mass is known; see e.g. ref 19) and implies that the accretion is (just) sub-Eddington. The breadth of the iron lines implies (using the methods of ref. 8) that the black hole has a high spin, of dimensionless spin parameter $a = cJ/M^2 > 0.98$, and so much of the emission should originate from within a few gravitational radii. Iron L-line emission should be detectable in similar sources²⁰ with high iron abundances, thereby enabling reverberation studies to be made.

References

- [1] Tanaka, Y. *et al.* Gravitationally Redshifted Emission Implying an Accretion Disk and Massive Black-Hole in the Active Galaxy MCG:-6-30-15. *Nature*. **375**, 659–661 (1995)
- [2] Nandra, K. *et al.* An XMM-Newton survey of broad iron lines in Seyfert galaxies. *Mon. Not. R. Astro. Soc.* **382**, 194–228 (2008)

- [3] Miller, J.M. Relativistic X-Ray Lines from the Inner Accretion Disks Around Black Holes. *Ann. Rev. Astro. & Astrophys.* **45**, 441–479 (2007)
- [4] Cackett, E.M. *et al.* Relativistic Iron Emission Lines in Neutron Star Low-Mass X-Ray Binaries as Probes of Neutron Star Radii. *Astrophys. J.* **674**, 415–420 (2008)
- [5] Guilbert, P.W. & Rees, M.J. ‘Cold’ material in non-thermal sources. *Mon. Not. R. Astro. Soc.* **233**, 475–484 (1988)
- [6] Ross, R.R. & Fabian, A.C. The effects of photoionization on X-ray reflection spectra in active galactic nuclei. *Mon. Not. R. Astro. Soc.* **261**, 74–82 (1993)
- [7] Fabian, A.C. *et al.* X-ray fluorescence from the inner disc in Cygnus X-1 *Mon. Not. R. Astro. Soc.* **238**, 729–736 (1989)
- [8] Brenneman, L.W. & Reynolds, C.S. Constraining Black Hole Spin via X-Ray Spectroscopy. *Astrophys. J.* **652**, 1028–1043 (2006)
- [9] Osterbrock, D. E.; Pogge, R. W., The spectra of narrow-line Seyfert 1 galaxies, **vol. 297**, 1985, 166–176 (1985)
- [10] Boller, Th. *et al.* XMM-Newton discovery of a sharp spectral feature at 7 keV in the narrow-line Seyfert 1 galaxy 1H 0707 - 49 *Mon. Not. R. Astro. Soc.* **329**, L1–L5 (2002).
- [11] Fabian, A.C. *et al.* X-ray reflection in the narrow-line Seyfert 1 galaxy 1H 0707-495 *Mon. Not. R. Astr. Soc.* **353**, 1071–1077 (2004)
- [12] Gallo, L.C. *et al.* Long-term spectral changes in the partial-covering candidate narrow-line Seyfert 1 galaxy 1H 0707-495. *Mon. Not. R. Astr. Soc.* **353**, 1064–1070 (2004)

- [13] Tanaka, Y. *et al.* Partial Covering Interpretation of the X-Ray Spectrum of the NLS1 1H 0707-495. *Pub. Astr. Soc. Japan.* **56**, L9–L13 (2004)
- [14] Laor, A. Line profiles from a disk around a rotating black hole. *Astrophys. J.* **376**, 90–94 (1991)
- [15] Ross, R. R.; Fabian, A. C., A comprehensive range of X-ray ionized-reflection models, *Mon. Not. R. Astr. Soc.* **358**, 211–216 (2005)
- [16] Shara, M.M. & Hurley, J.R. Star Clusters as Type Ia Supernova Factories. *Astrophys. J.* **571**, 830–842 (2002)
- [17] Uttley, P., McHardy, I. M., Vaughan, S., Non-linear X-ray variability in X-ray binaries and active galaxies, *Mon. Not. R. Astr. Soc.* **359**, 345–362 (2005)
- [18] Arvalo, P., Uttley, P., Investigating a fluctuating-accretion model for the spectral-timing properties of accreting black hole systems, *Mon. Not. R. Astr. Soc.* **367**, 801–14 (2006)
- [19] Bian, W., Zhao, Y., On X-ray variability in narrow line and broad line active galactic nuclei, *Mon. Not. R. Astr. Soc.* **343**, 164–168 (2003)
- [20] Gallo, L. Investigating the nature of the narrow-line Seyfert 1 galaxies with high-energy spectral complexity, *Mon. Not. R. Astr. Soc.* **368**, 479–486 (2006)

1 Acknowledgements

ACF thanks the Royal Society for support. This work is based on observations made with *XMM-Newton*, an ESA science mission with instruments and contributions directly funded by ESA member states and the USA (NASA). AZ acknowledges the support of the Algerian Higher Education Ministry and STFC. CSR, WNB GM, GP and both RCR and AJB acknowledge support from the US National Science Foundation, NASA, the Spanish Ministerio de Ciencia e Innovación, Italian ANR and UK STFC for support, respectively.

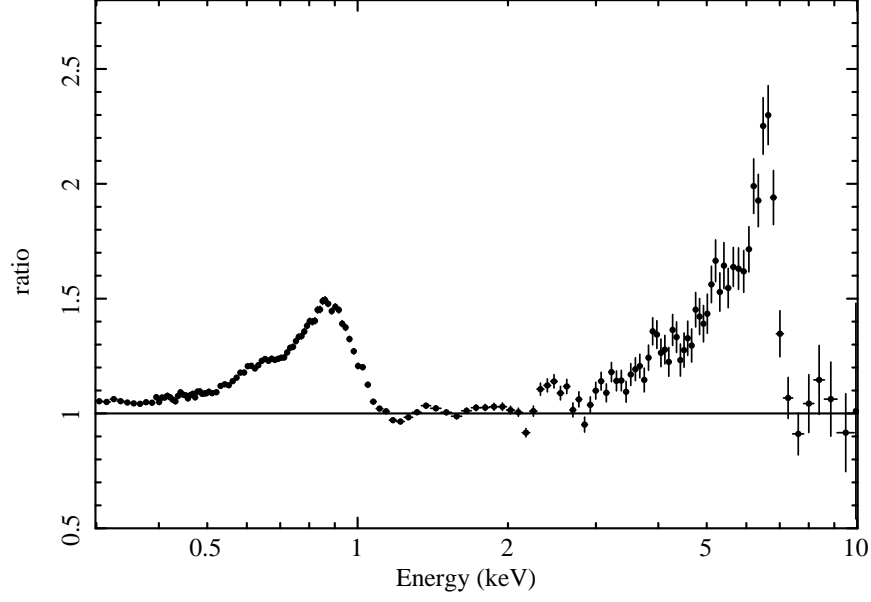


Figure 1: Ratio of the spectrum, obtained by combining all 4 XMM orbits, to a simple phenomenological model composed of a power-law, blackbody and 2 broad emission lines. The normalizations of the broad lines have been set to zero to make this plot. Ionized iron-L and K peak in the rest frame around 0.9 keV and 6.5-6.7 keV with equivalent widths of 180 and 970 eV, respectively.

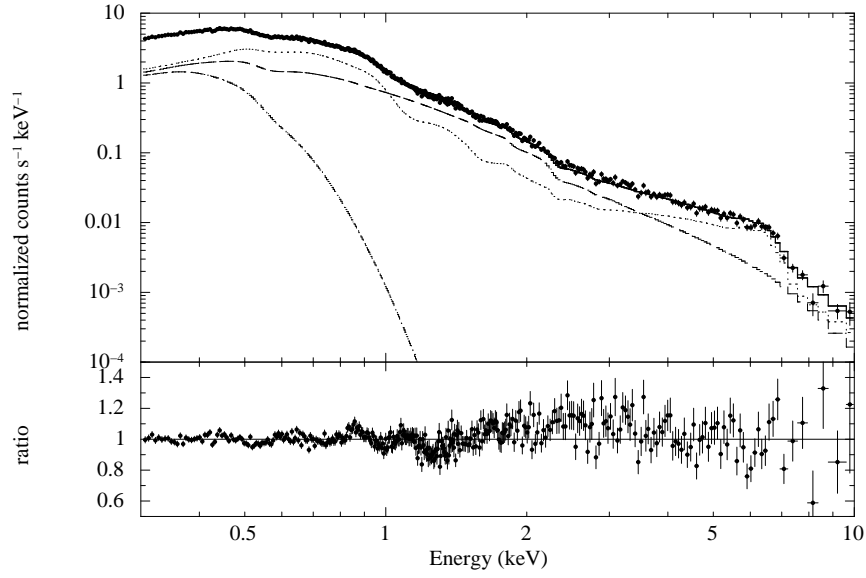


Figure 2: Spectrum of the first orbit showing the best-fitting, self-consistent, relativistically-blurred, reflection model. The total exposure time for this spectrum is 102 ks with the source changing flux continuously and by more than a factor of 2 every few ks. The offset in the 1.5–4 keV band is due to the simplicity of using just two components in the 1–10 keV band despite the high variability of the source. The addition of a further reflection component with higher ionization parameter considerably reduces this offset (see the Supplementary Information for more details). This is to be expected if the ionization changes with time or flux. The contributions of the power-law, reflection and blackbody components are indicated by the dashed, dotted and dash-dotted lines respectively.

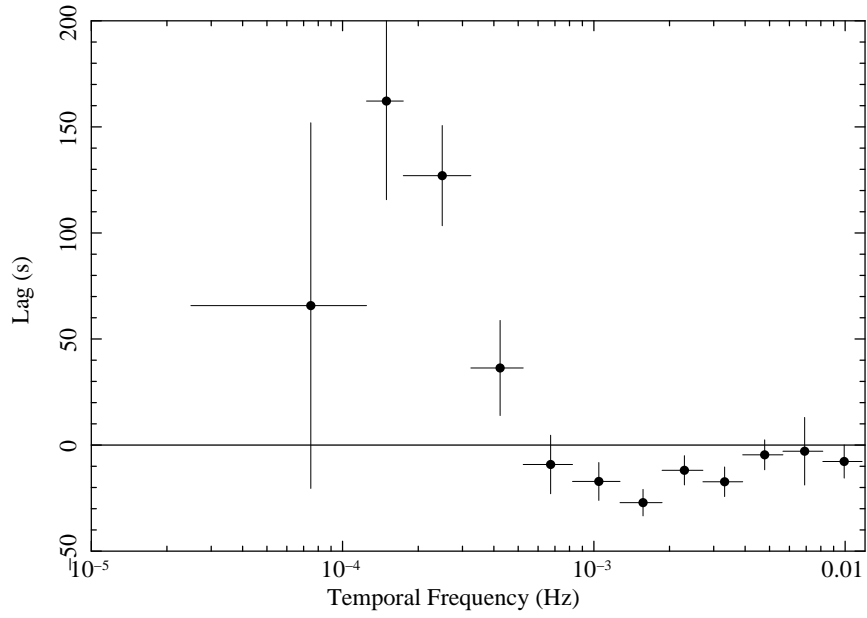


Figure 3: Frequency-dependent lags between the 0.3–1 and 1–4 keV bands. A negative lag, such as found above frequencies of 7×10^{-4} Hz or timescales shorter than 30 min, indicates the harder flux, dominated by the powerlaw continuum, changing before the softer flux, which is dominated by reflection (particularly the iron L line).

2 Supplementary Information

1H0707-495 was observed for four consecutive orbits using XMM-Newton starting on 2008, January 29th. The observations were made in the large window imaging mode. The data were analysed using XMM Science Analysis System (SAS v8.0.0). The light curve was filtered to remove any background flares, and resulted in a total net exposure of 330 ks for the EPIC PN camera. No significant pileup was found in the patterns, which were selected using $\text{PATTERN} \leq 4$. Source spectra were extracted from circular regions with a radius of 35 arcsec around the source, and background spectra from regions on the same chip. The spectra were then grouped to bins with a minimum of 20 counts each. The response matrices were generated using RMFGEN and ARFGEN in SAS. For the combined spectrum of the four orbits, the events files were merged together before extracting the spectrum.

The light curve is shown (Fig. 4), together with the FeL line profile as seen by the RGS (Fig. 6). No significant sharp absorption features are seen around 1 keV in the RGS spectrum; Chandra HEG spectra have tentatively shown features in this band (Leighly et al 2002). The ratio plot for each orbit (Fig. 5), produced in a similar way to Fig. 1, is also shown, as well as the difference spectrum (Fig. 7). This spectrum fits a power-law above 1.1 keV and has a significant excess at lower energies and a marginal excess from 4–7 keV; it is consistent within the error bars with the difference spectrum in Ref. 11. We assume that the excesses are due to small changes in the ionization parameter of the irradiated disc (sample fits indicate that ξ changes by about 20 per cent between orbits). This also accounts for changes in the iron-L to K line ratio between the orbits.

Fitting the data with a simple model consisting of 2 broad lines, a power-law continuum and a low energy blackbody spectrum gives the following parameters for the lines (assuming a Laor model and with uncertainties at the 90% confidence level): K-line energy (our frame) $6.19^{+0.11}_{-0.14}$ keV, L-line energy $0.864^{+0.010}_{-0.012}$ keV, $r_{\text{in}} = 1.39^{+0.07}_{-0.01} r_g$, disc inclination $55.7^{+0.6}_{-1.1}$ deg, emissivity index $5.8^{+0.16}_{-0.26}$, r_{out} fixed at $400 r_g$ and photon index $\Gamma = 2.87^{+0.02}_{-0.01}$.

The best-fitting reflection model spectrum is shown (Fig. 8). This spectrum has soft X-ray absorption due to a column of $8.7 \times 10^{20} \text{ cm}^{-2}$ (the Galactic column density in that direction is $5 \times 10^{20} \text{ cm}^{-2}$ so we assume that there is some excess in the host galaxy). The emission spectrum has a power-law (photon index of 3.09) plus low energy blackbody continuum ($kT = 52 \text{ eV}$) components and a relativistically blurred reflection component (reflionx¹⁵) with iron at 8.88 times the Solar value and an ionization parameter of 53.4. The power-law has the same photon index as for the reflection model, where it extends down to 0.1 keV. The blurring is for an inner disc radius of $1.235 r_g$, and an emissivity index of 7.43 breaking at $4.32 r_g$ to an index of 1.93. The disc inclination is 53.4 deg. Note that the blackbody component, presumably thermal disc emission, only makes a significant contribution below 0.5 keV and has a temperature about one third of that typically invoked for phenomenological models for AGN (Crummy et al 2007 and references therein).

Adding a second reflection component with the same set of parameters as the first, except for a higher ionization parameter in the range of 500–1200, gives a better fit with the residuals in the 1.5–4 keV band (Fig. 10). Future work will address whether this is due to source variability, to an intrinsic range of ionization, or to spatial inhomogeneity of the reflector.

Phenomenological absorption models, such as those discussed and fitted above 2 keV to earlier data in Refs. 10 and 12, can fit the new data. However the strong feature around 1 keV requires a broad emission line, which implies reflection. An iron-L edge predicts other features (UTAs) which are inconsistent with the data.

We plot the ratio of the data to a power-law continuum of photon index 3 in Fig. 9 and the rms variability spectrum in Fig. 11.

The mean high-frequency lag (above $7 \times 10^{-4} \text{ Hz}$) between the 0.5–1 and 3–7 keV bands is $-6 \pm 18 \text{ s}$, indicating that the iron-L and K features vary together, as expected for reflection.

The NLS1 IRAS 13224-3809 shows a similar pair of FeK and FeL lines (Ponti et al in prep).

References

- [1] Crummy, J.C., Fabian, A.C., Gallo, L., Ross, R.R., *An explanation for the soft X-ray excess in active galactic nuclei*, *Mon. Not. R. Astro. Soc.*, 365, 1067–1081 (2006)
- [2] Leighly, K.M., Zdziarski, A.J., Kawaguchi, T., Matsumoto, C., *A Chandra observation of the luminous NLS1 1H0707-495*, Workshop Proceedings, MPE report, eds T. Boller et al, Garching (2001)

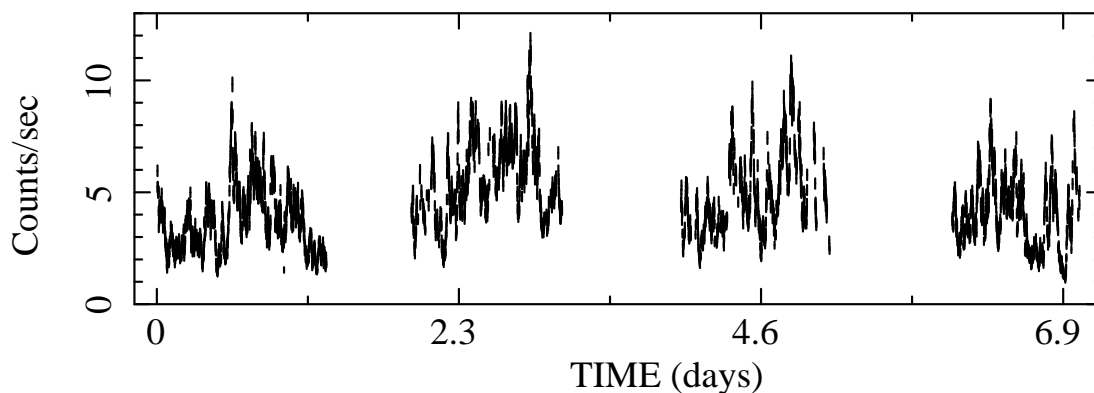


Figure 4: Total light curve (0.3–10 keV) of the XMM observation showing all 4 orbits.

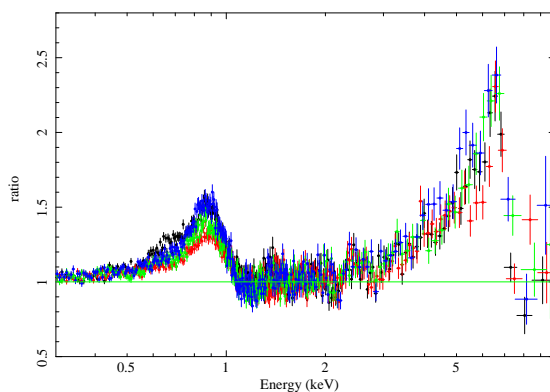


Figure 5: Ratio of the spectral data from each XMM orbit to a simple phenomenological model composed of a power-law, blackbody and 2 broad emission lines. The normalizations of the broad lines have been set to zero to make this plot. Ionized iron-L and K peak in the rest frame around 0.9 keV and 6.5-6.7 keV, respectively.

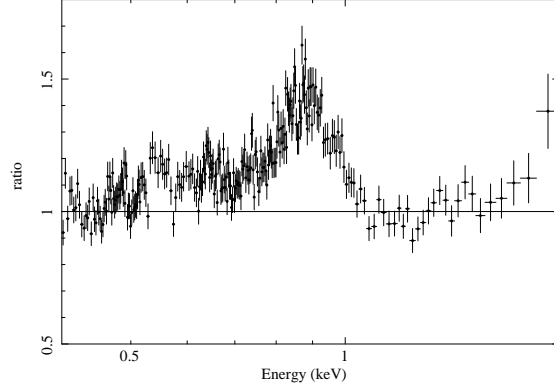


Figure 6: Ratio spectrum from the XMM reflection grating spectrometer (produced as for Fig. 1). We find no significant sharp features in this spectrum around 1 keV.

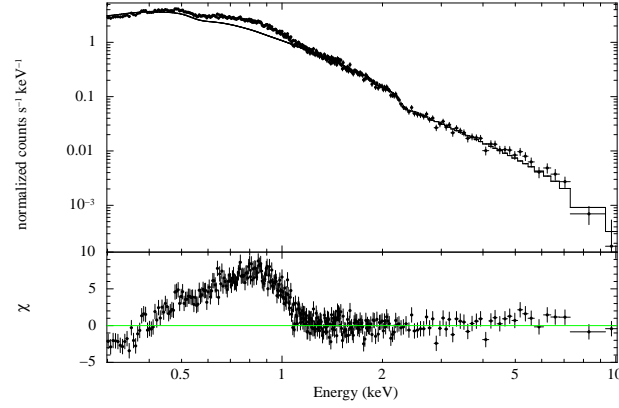


Figure 7: The difference spectrum for all 4 orbits (i.e. the spectrum formed by subtracting the fainter half of the spectra from the brighter half) fitted with a simple power-law spectrum with Galactic absorption.

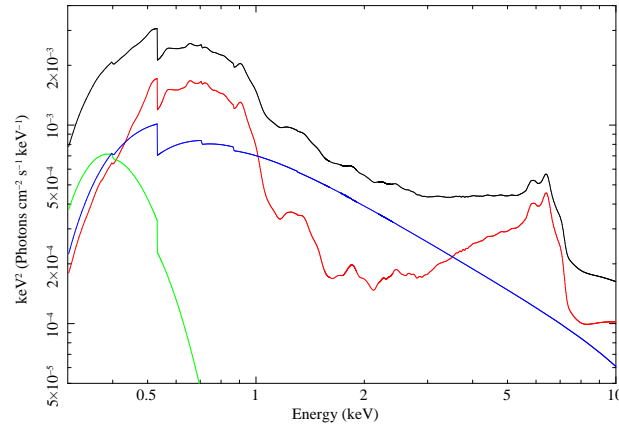


Figure 8: Best-fitting reflection model spectrum (see text for details), with components shown.

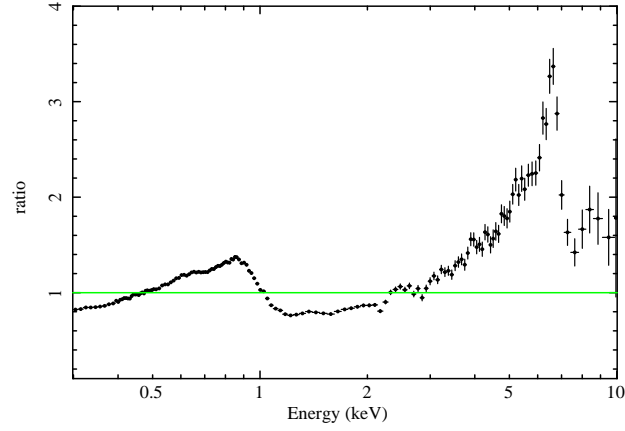


Figure 9: Ratio of the total spectrum to a powerlaw of photon index $\Gamma = 3$.

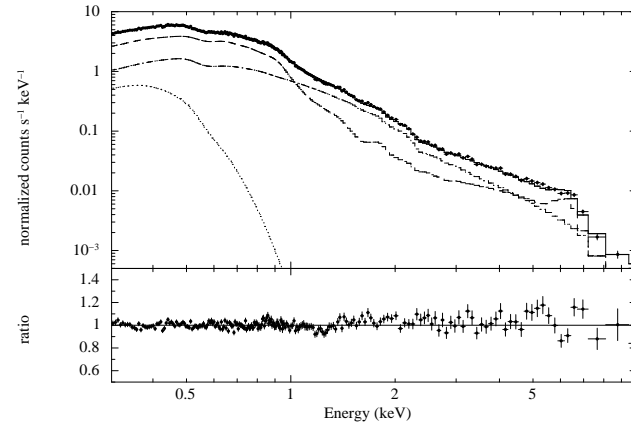


Figure 10: Similar spectrum to Fig. 1 but with an additional reflection component (shown summed with the first one) with ionization parameters $\xi = 528$ and 997 . Note that neither this spectrum, nor any of the other spectra, has been unfolded.

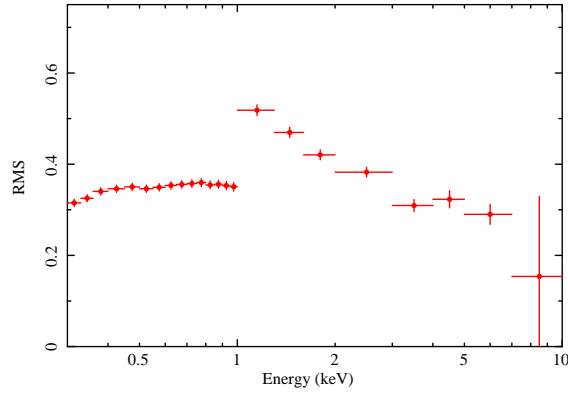


Figure 11: RMS variability spectrum.